TG–1008
AUGUST 1968
Copy No. 105

AD 676503

Technical Memorandum

TEMPERATURE FUNCTIONS FOR OGIVAL RADOME THERMAL-STRESS ANALYSIS

by MANFORD B. TATE

OCT 24 1968

THE JOHNS HOPKINS UNIVERSITY • APPLIED PHYSICS LABORATORY

This document has been approved for public release and sale; its distribution is unlimited.

Reproduced by the
CLEARINGHOUSE
for Federal Scientific & Technical
Information Springfield Va. 22151

TG–1008
AUGUST 1968

Technical Memorandum

TEMPERATURE FUNCTIONS FOR OGIVAL RADOME THERMAL-STRESS ANALYSIS

by MANFORD B. TATE

THE JOHNS HOPKINS UNIVERSITY ▪ APPLIED PHYSICS LABORATORY
8621 Georgia Avenue, Silver Spring, Maryland 20910

Operating under Contract NOw 62-0604-c with the Department of the Navy

This document has been approved for public release and sale; its distribution is unlimited.

THE JOHNS HOPKINS UNIVERSITY
APPLIED PHYSICS LABORATORY
SILVER SPRING, MARYLAND

ABSTRACT

Nine temperature functions are required in finding thermal stresses in the mainbody of a bicentric-ogive radome; and seven, in the nosecap. They are formulated and collected in this report for future use in numerical analysis. Included among these functions are:

(1) Spanwise distribution of temperature along the outer surface of the radome,

(2) Temperature distribution through the thickness of the radome wall,

(3) Zonal distributions of thermal strain,

(4) Thermal normal-stress resultants,

(5) Thermal bending-moment resultants,

and they are discussed, exemplified, and evaluated numerically in the body of the text.

THE JOHNS HOPKINS UNIVERSITY
APPLIED PHYSICS LABORATORY
SILVER SPRING MARYLAND

TABLE OF CONTENTS

LIST OF FIGURES

THE JOHNS HOPKINS UNIVERSITY
APPLIED PHYSICS LABORATORY
SILVER SPRING, MARYLAND

I. INTRODUCTION

Reports that provide fundamental information preparatory to radome thermal-stress analysis were published as References (1) to (7), inclusive. General relations for surface temperatures were developed in Reference (1), and geometric expressions used in test-data reduction were obtained in Reference (2). Wind-tunnel experimental results and heat-transfer analyses were correlated in Reference (3) and supplied empirical coefficients for use in the Reference (1) formulas.

Temperature-dependent material properties and measured thermal expansions of Pyroceram 9606 were put into functional forms in Reference (4). And in Reference (5) it was shown how compound-ogives can be substituted for the Von Karman configuration that was tested aerodynamically.

A theoretical solution was derived in Reference (6) for thermal stress in an ogival radome whose wall has heat-variant material properties and nonlinear thermal expansion during axisymmetrical heating by rapid flight through the air. Approximation functions to particular solutions in the Reference (6) theory were presented in Reference (7).

In the present report, the different kinds of temperature functions that occur in the analysis described in Reference (6) are obtained, exemplified, and evaluated. They are evolved from the basic information given in References (1) to (7), inclusive.

II. NOMENCLATURE

A,B,C:	Constants
D:	Wall stiffness factor, $D = Eh^3/12(1-\nu^2)$
E:	Young's modulus of elasticity, psi
I:	Moment of inertia, $I = h^3/12$
J,K:	Constants
L:	An operator
M:	Moment resultant, ippi
N:	Normal-stress resultant, ppi
P:	Constant
Q:	Shearing-stress resultant, ppi
R:	Spatial radius, inches
T:	Temperature, °F
V:	Change of wall slope, radians
Z:	Geometric axis of a radome
a,b:	Series coefficients
c:	Half-thickness of wall (c=h/2), inches
e:	Normal strain, ipi
h:	Wall thickness, inches
i,j:	Positive integers
ℓ:	Length, inches
m,n:	Positive integers
q:	Auxiliary shear function, ppi
r:	Planar radius, inches
u,w:	Displacement functions, inches
x:	Thickness-variable ratio, x = y/c
y:	Thickness coordinate, inches
z:	Coordinate along geometric axis, inches
β:	Wall-bending parameter, radians
ϵ:	Normal strain, ipi
θ:	Coordinate angle of rotation, radians or degrees
ν:	Poisson's ratio
σ:	Normal stress, psi
χ:	Curvature change, radians per inch
ψ:	Coordinate angle of azimuth, radians or degrees
R,θ,ψ:	Spherical coordinates
r,θ,z:	Cylindrical coordinates

The following notations appear as subscripts:

a:	Anterior or outer surface
c:	Central surface
i,j,m,n:	Indices associated with counters i,j,m,n, respectively
o:	Origin or initial value (zero)
s:	Secondary or inner surface
t:	Thermal
R,θ,ψ:	Spherical-coordinate directions
r,θ,z:	Cylindrical-coordinate directions

III. TEMPERATURE DISTRIBUTION

1. GENERAL TEMPERATURE FORMULA

(a) Experimental Results - A wall profile of the ogive shape is shown in Figure 1 and a spherical segment as a nosecap in Figure 2. From the results given in References (1), (2), and (3), it was found that the temperature T at any point in the radome wall or at its inner and outer surfaces can be expressed by

$$T = T(x,\psi) = f(x)T_a(\psi) \tag{1}$$

where f is the thickness distribution function, and T_a represents temperatures along the outer surface of the radome.

(b) Wall-Thickness Distribution - As developed in Reference (3), the function f that describes the temperature distribution through the thickness of the radome wall is given by

$$f(x) = \sum_{n=0}^{3} f_n x^n = 0.257 + 0.358x + 0.305x^2 + 0.084x^3 \tag{2}$$

which defines a third-order nonlinear distribution through the wall thickness.

(c) Exterior-Surface Temperature - The temperature along the outer surface of a radome was studied in References (1) and (3) with the aid of Reference (2). It was learned that the distribution was dependent on the coordinate angle of azimuth ψ, and

$$T_a = T_a(\psi) \tag{3}$$

where, in general, T_a is a highly nonlinear function of the variable angle. The relations are illustrated in Figure 3 and discussed in the next section.

2. OUTER-SURFACE SPANWISE TEMPERATURE DISTRIBUTIONS

(a) Experimental Distribution - The spanwise distribution of temperature at the radome's exterior surface is shown in Figure 3. The plotted points were calculated with semiempirical regression formulas developed in Reference (3). On the bicentric-ogive structure described in Reference (5), the temperature distribution was then imposed within two percent by means of the four nonlinear expressions that are written on the figure and appear as solid-line curves.

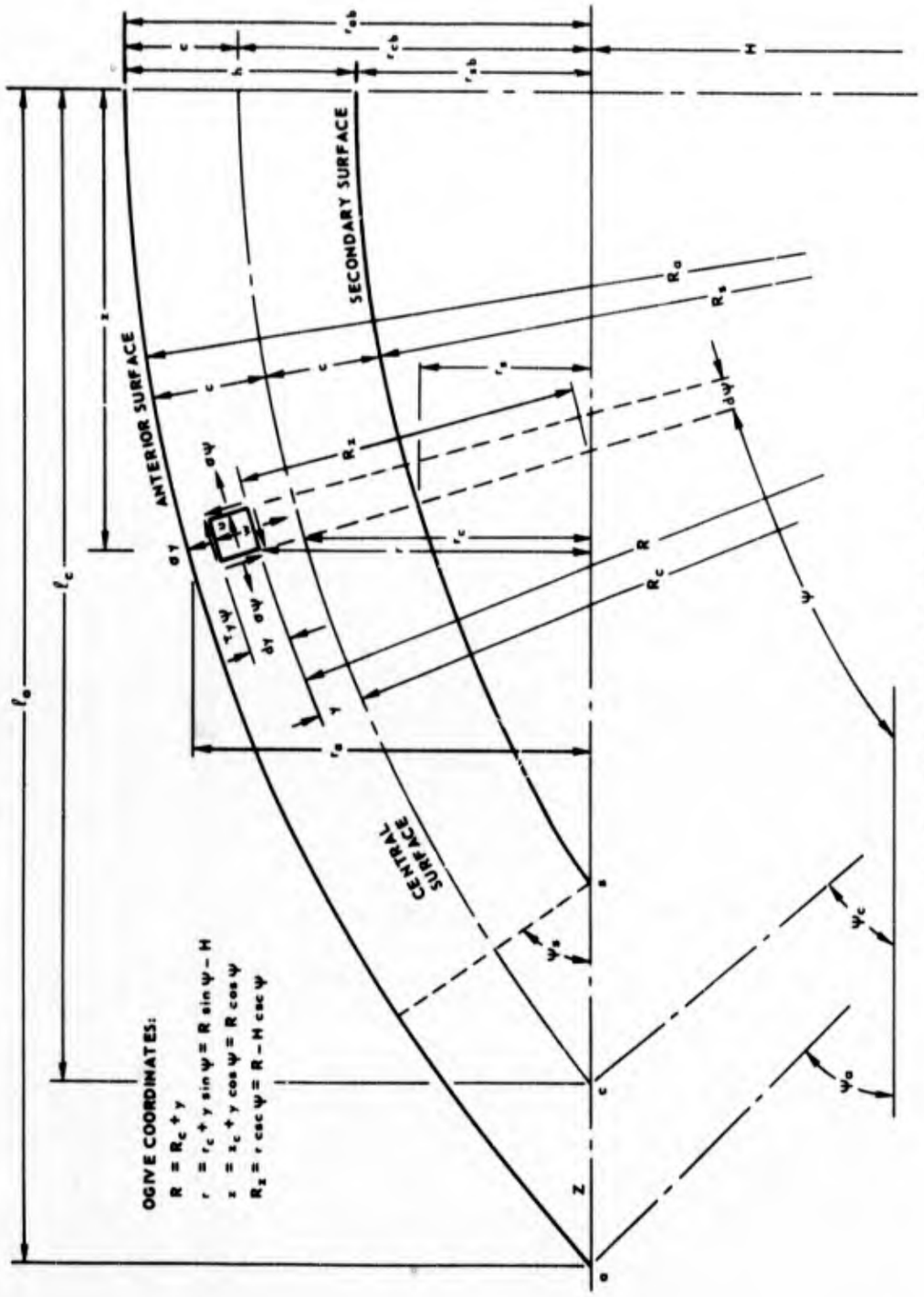

Fig. 1 OGIVAL RADOME WALL DIMENSIONS

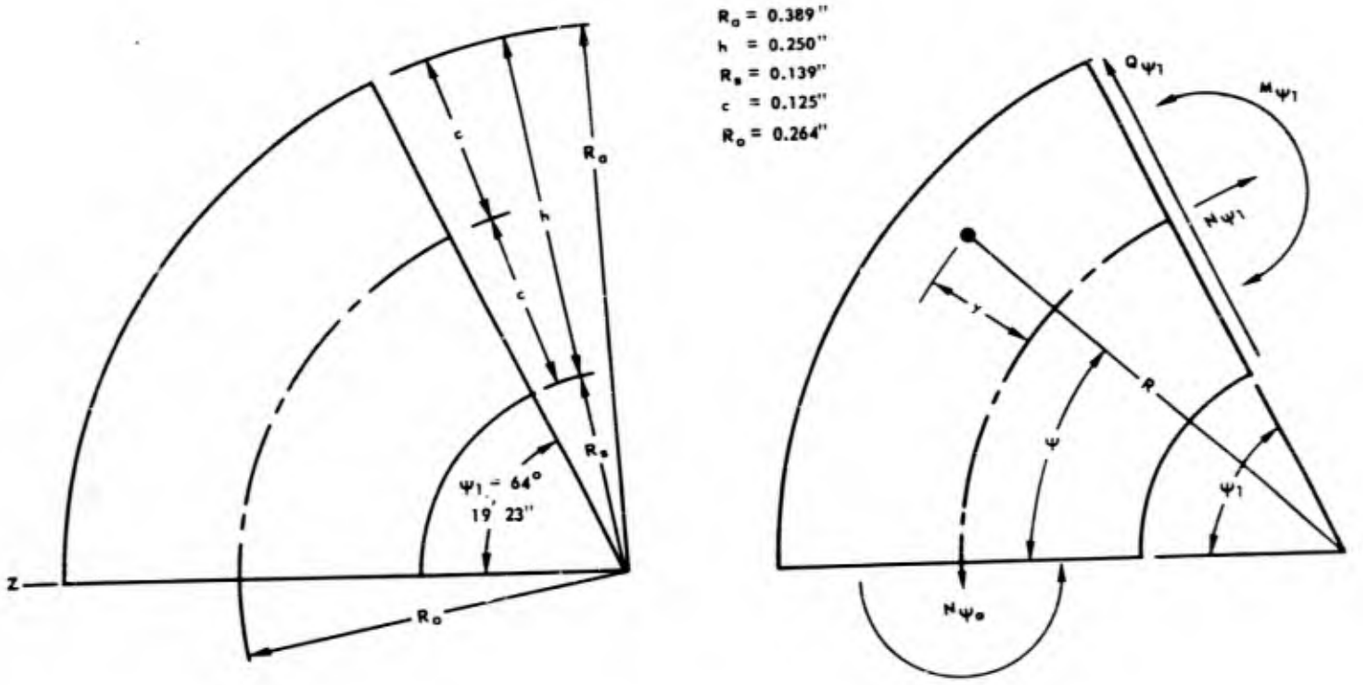

Fig. 2 NOSECAP DIMENSIONS AND RESULTANTS

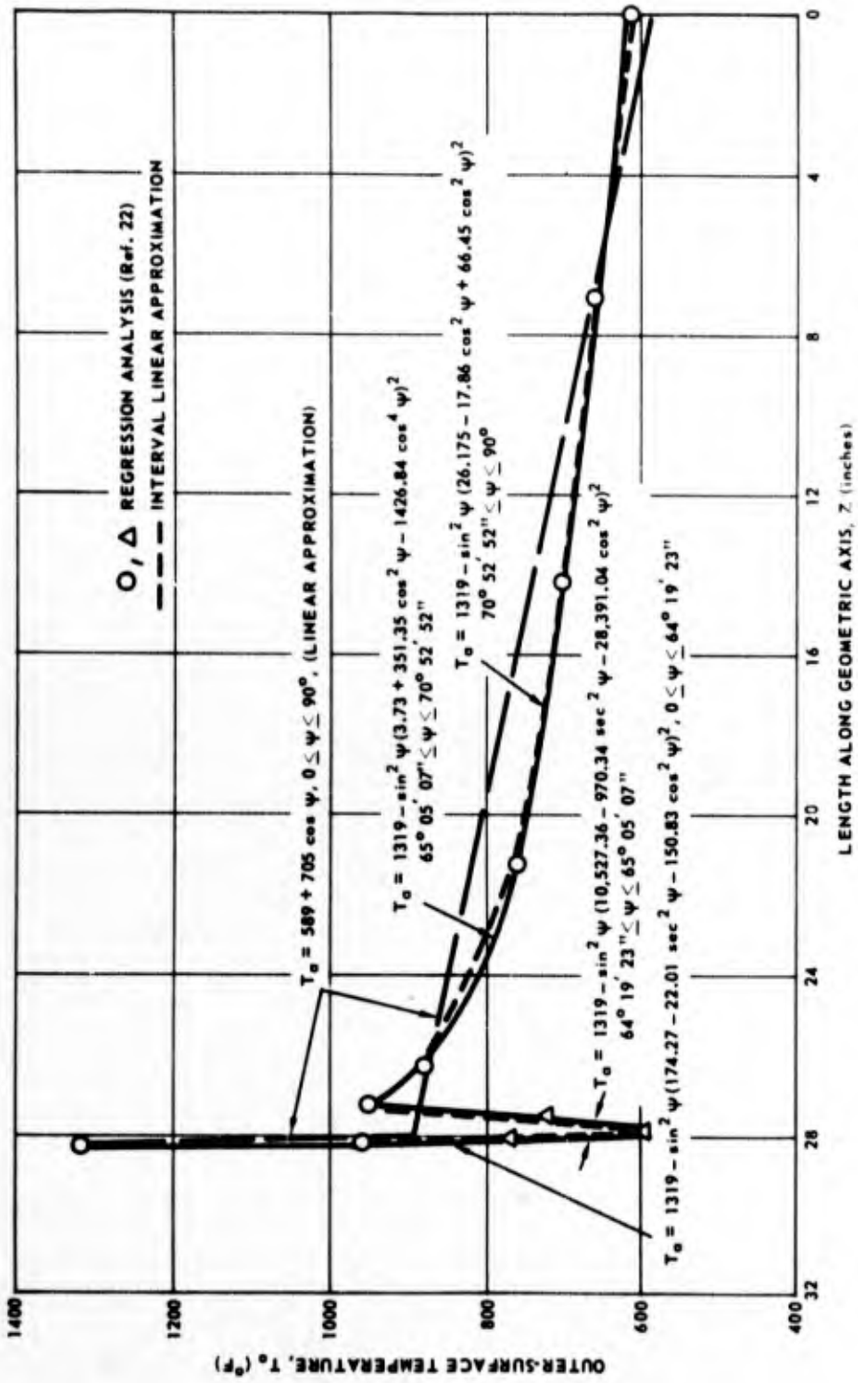

Fig. 3 SPANWISE TEMPERATURE DISTRIBUTION FOR BICENTRIC-OGIVE RADOME

(b) Full-Span Linear Approximation - Also given in Figure 3 is a straight-line approximation of the temperature distribution over the entire span. It was computed as

$$T_a = 589 + 705 \cos\Psi \tag{4}$$

and is shown as the long-dashed line in the figure. Furthermore, this full-span linear approximation is employed in the calculations that are reported herein.

(c) Piecewise Linear Approximations - When the exterior-surface temperatures (T_a) are represented by piecewise linear approximations along the span, the equation for the ijth interval is:

$$T_a = T_{oij} + T_{1\,ij} \cos\Psi, \qquad \Psi_i \le \Psi \le \Psi_j \tag{5}$$

where T_{oij} and $T_{1\,ij}$ are interval constants. Index "i" denotes the beginning and "j" the end of each successive interval of approximation. These relations are indicated by the short-dashed lines on Figure 3, and the constants are listed in Table 1.

Table 1. Constants for Piecewise Linear Approximation of T_a.

z_a (in.)	Ψ (deg-min-sec)	i	j	T_{oij} (°F)	$T_{1\,ij}$ (°F)
28.3	0	0	--	+ 347	+ 972
28.0795	64-19-23	1	1	-27,076	+64,260
27.9	64-29-56	2	2	+17,329	-38,881
27.3	65-05-07	3	3	- 961	+ 4,536
26.3	66-03-22	4	4	+ 258	+ 1,532
21.225	70-52-52	5	5	+ 583	+ 540
14.15	77-23-16	6	6	+ 623	+ 357
7.075	83-43-57	7	7	+ 625	+ 339
0	90	-	8	+ 625	+ 339

The tabulated constants were computed with the general expressions

$$T_{1\,ij} = \frac{T_{ai} - T_{aj}}{\cos\Psi_i - \cos\Psi_j}, \qquad T_{oij} = T_{ai} - T_{1\,ij} \cos\Psi_i \tag{6}$$

and illustration of their application follows.

In the first interval (ij = 01), the linear approximation extends from the tip (ψ=0) to the end of the nosecap, where $\psi = \psi_1 = 64°19'23"$ as sketched in Figure 2. The surface temperature straight-line equation for this segment is

$$T_a = 347 + 972 \cos\psi, \quad 0 \leq \psi \leq 64°19'23" \tag{7}$$

and the preceding equation yields the plotted-data values at the beginning and end of the interval (1319°F and 768°F, respectively, as plotted on Figure 3). For intervals between the quarter and mid points of the span, the linearized expressions are:

$$T_a = 583 + 540 \cos\psi, \quad 70°52'52" \leq \psi \leq 77°23'16" \tag{8}$$

$$T_a = 623 + 357 \cos\psi, \quad 77°23'16" \leq \psi \leq 83°43'57" \tag{9}$$

and the foregoing relations can be adapted for numerical analysis in the manner that is used subsequently with the full-span linear temperature distribution, equation (4).

IV. TEMPERATURE FUNCTIONS

1. THERMAL STRAIN

(a) Experimental Results - The thermal-strain (ϵ_t) functions are obtained from the Pyroceram 9606 test data investigated in Reference (4). Thermal expansion of this material nonlinearly increases with increasing temperature; and, by examination of the temperature distribution in the Von Karman test radome, which was reported in Reference (3), we learned that the Pyroceram thermal strain is advantageously expressed as follows:

$$\epsilon_t = (-241.2 + 3.445T) \times 10^{-6}, \quad 70° \leq T \leq 400°F \tag{10}$$

$$= (-119.1 + 2.958T) \times 10^{-6}, \quad 200° \leq T \leq 600°F \tag{11}$$

$$= (+190.3 + 2.221T) \times 10^{-6}, \quad 300° \leq T \leq 1400°F \tag{12}$$

wherein T is given by equation (1). Owing to the presence of f(x) in T, the three expressions for deformation, equations (10), (11), and (12), permit great simplification in numerical analysis as explained in the next paragraph.

Inspection of the distribution of temperature defined throughout the radome by equations (1), (2), and (3) revealed that the equation (10) temperature limits apply to the inside half of the wall ($-1 \leq x \leq 0$) along the entire span, those for equation (11) define T over the full span in the quarter thickness above the wall centerline ($0 \leq x \leq 0.5$), and (12) serves the same purpose in the outer quarter of the wall thickness ($0.5 \leq x \leq 1$). This arrangement expedites the calculation of integrals for thermal normal stress and moment resultants.

(b) Zonal Approximations - The three ϵ_t expressions are thought of as zonal functions. Strains computed with equation (10) agree with measured data, Reference (4), within -1 to +3 percent. Those calculated from (11) correspond to the measurements within five percent; and the ones from (12) agree within ±7 percent in the low part of the temperature range, which is used but slightly, and deviations in the upper half of the temperature range lie approximately between -2 and +4 percent.

2. MATERIAL PROPERTIES OF PYROCERAM 9606

(a) Poisson's Ratio - As pointed out in Reference (4), Poisson's ratio ν is nearly constant for the Pyroceram 9606 material. Between 70°F and 2460°F, measured values were reported between 0.237 and 0.250. If we use a mean value of 0.244 between 70°F and 1400°F, the largest differences between this mean value and the test data amount to ±2.5 percent. Therefore, we shall employ the constant shown below.

$$\nu = 0.244, \qquad 70^\circ \leq T \leq 1400^\circ F \tag{13}$$

Since the preceding value was found by balancing the maximum positive and negative differences, equation (13) represents ν with substantially less than 2.5 percent error at most points in the radome.

(b) Young's Modulus - If we were to use mean values of Young's modulus of elasticity in the temperature ranges of the thermal-expansion functions, equations (10), (11), and (12), they would be

$$E = 16.07 \times 10^6 \text{ psi}, \qquad 70^\circ \leq T \leq 400^\circ F \tag{14}$$

$$= 16.34 \times 10^6 \text{ psi}, \qquad 200^\circ \leq T \leq 600^\circ F \tag{15}$$

$$= 16.64 \times 10^6 \text{ psi}, \qquad 300^\circ \leq T \leq 1400^\circ F \tag{16}$$

as calculated with data reported in Reference (4). But one might also use the following mean value over the entire range of temperatures.

$$E = E_{av} = 16{,}400{,}000 \text{ psi}, \qquad 70^\circ \leq T \leq 1400^\circ F \tag{17}$$

The differences between test values and elastic modulus (14) are ±2 percent; for modulus (15), ±2.2 percent; for (16), ±2.7 percent; and approximately ±4 percent for modulus (17). Inasmuch as the percentages just quoted are proportional to maximum deviations, and differences in about 80 to 90 percent of each range of temperatures are sensibly less than the quoted maxima, the net effect on the computed stresses and displacements will probably be in the order of one-half of the given percentages. Furthermore, it appears likely that use of constant (13) for Poisson's ratio will only affect the final results slightly.

3. THERMAL NORMAL-STRESS RESULTANTS

(a) Mainbody - With the thermal normal-stress resultants defined by the integrals given in Reference (6), ν and E the constants of equations (13) and (17), ϵ_t from equations (10) to (12), and T from equations (1) to (4), inclusive, the functions are found to be

$$N_{t\theta} = \int_{-c}^{+c} \frac{RE\epsilon_t dy}{(1-\nu)R_c} = K_o + K_1 \cos\psi \tag{18}$$

$$N_{t\psi} = \int_{-c}^{+c} \frac{rE\epsilon_t dy}{(1-\nu)r_c} = N_{t\theta} + (K_2 + K_3 \cos\psi)R_c/r_c \tag{19}$$

in which the K_i are constants as shown next.

$$K_o = 4.648Eh/(1-\nu) \times 10^4, \qquad K_1 = 6.792Eh/(1-\nu) \times 10^4 \tag{20}$$

$$K_2 = 4.393Eh/(1-\nu) \times 10^7, \qquad K_3 = 3.420Eh/(1-\nu)10^7 \tag{21}$$

The radii r_c and R_c that occur in equations (18) and (19) are illustrated in Figure 1 and defined by relations shown on the same figure.

(b) Nosecap - When obtained similarly for the nosecap, the normal-stress resultant temperature functions are equal; i.e.,

$$N_{t\psi} = N_{t\theta} = N_t = \int_{-c}^{+c} \frac{RE\epsilon_t dy}{(1-\nu)R_o} = K'_o + K'_1 \cos\psi \tag{22}$$

$$K_o' = 5.842Eh/(1-\nu) \times 10^4, \quad K_1' = 7.722Eh/(1-\nu) \times 10^4 \tag{23}$$

and the equality shown by (22) is brought about because $R/R_c = r/r_c = R/R_o$ in the nosecap alone.

4. THERMAL BENDING-MOMENT RESULTANTS

(a) Mainbody - With the thermal bending moments defined by integrals given in Reference (6), ν and E the constants of equations (13) and (17), ϵ_t from equations (10) to (12), and T from equations (1) to (4), inclusive, the moment temperature functions are found to be

$$M_{t\theta} = \int_{-c}^{+c} \frac{RE\epsilon_t y dy}{(1-\nu)R_c} = J_o + J_1 \cos\psi \tag{24}$$

$$M_{t\psi} = \int_{-c}^{+c} \frac{rE\epsilon_t y dy}{(1-\nu)r_c} = M_{t\theta} + (J_2 + J_3 \cos\psi)R_c/r_c \tag{25}$$

in which the J_i are constants as shown next.

$$J_o = 1.269Eh^2/(1-\nu) \times 10^4, \qquad J_1 = 0.989Eh^2/(1-\nu) \times 10^4 \tag{26}$$

$$J_2 = 1.704Eh^2/(1-\nu) \times 10^7, \qquad J_3 = 2.195Eh^2/(1-\nu) \times 10^7 \tag{27}$$

One can see that the K_i have the dimensions of pounds per inch (ppi); and the J_i, of inch-pounds per inch (ippi).

(b) Nosecap - When obtained similarly for the nosecap, the bending-moment temperature functions are equal; i.e.,

$$M_{t\psi} = M_{t\theta} = M_t = \int_{-c}^{+c} \frac{RE\epsilon_t y dy}{(1-\nu)R_o} = J_o' + J_1' \cos\psi \tag{28}$$

$$J_o' = 1.732Eh^2/(1-\nu) \times 10^4, \qquad J_1' = 1.585Eh^2/(1-\nu) \times 10^4 \tag{29}$$

and the equality shown by (28) again is brought about because $R/R_c = r/r_c = R/R_o$ in the nosecap.

V. DISCUSSION

Temperature functions that are required in the analysis of radome-wall stresses are developed on the preceding pages. These include the temperature distributions of equations (1) to (9), inclusive, for which spanwise distributions are pictured in Figure 3.

Thermal strains are computed with equations (10) to (12), inclusive, and provide zonal approximations that are generally satisfactory.

By means of the distribution and strain functions, the thermal normal-stress and moment resultants are obtained for both mainbody and nosecap. In the examples, these resultants vary with $\cos\psi$ and R_c/r_c, which is also a function of the coordinate angle with $r_c = R_c\,(\sin\psi - \sin\psi_c)$.

All of these expressions are required in future numerical analyses of thermal stress and deformation.

VI. CONCLUDING REMARKS

Inasmuch as nine temperature functions are needed to compute thermal stresses in ogival radomes, they are formulated herein preparatory to their application in numerical analyses. The fundamental relations that underlie the expressions are discussed in References (1) to (7), inclusive.

REFERENCES

1. M. B. Tate, "Air Properties and Flow Conditions Around the Nose of a Blunt Radome," APL/JHU TG-981, 1968.

2. _____, "Curvature Radii and Derivatives for Thermal-Stress Analysis of Von Karman Radomes," APL/JHU TG-982, 1968.

3. _____, "Statistical Analysis of Temperature Data from Wind Tunnel Test of a Von Karman Radome," APL/JHU TG-983, 1968.

4. _____, "Functionalization of Pyroceram 9606 Test Data for Radome Thermal-Stress Analysis," APL/JHU TG-980, 1968.

5. _____, "Compound-Ogive Radomes as Substitute Structures for Von Karman Shapes," APL/JHU TG-985, 1968.

6. _____, "Axisymmetric Thermal Stresses in Ogival Radome Walls Having Material Properties that Change with Heat Intensity," APL/JHU BBE EM-3976, 1965.

7. _____, "Approximation Functions as Particular Solutions in Thermal-Stress Analysis of an Ogival Radome," APL/JHU TG- , 1968.

INITIAL DISTRIBUTION EXTERNAL TO THE APPLIED PHYSICS LABORATORY*

The work reported in TG-1008 was done under Navy Contract NOw 62-0604-c. This work is related to Task A33, which is supported by NAVORDSYSCOM.

ORGANIZATION	LOCATION	ATTENTION	No. of Copies
DEPARTMENT OF DEFENSE			
DDC	Alexandria, Va.		20
Department of the Navy			
NAVORDSYSCOM	Washington, D. C.	ORD-9132	2
		ORD-03511	1
NAVPLANTREPO	Silver Spring, Md.		1
Centers			
Naval Ship Research & Development Center	Annapolis, Md.	H. [illegible]. Koch	1
Laboratories			
NOL	White Oak, Md.	V. F. DeVost	1
		Dr. A. E. Seigel	1
		A. M. Corbin	1
		R. Mead	1
		G. Stathopoulos	1
		E. Rzepka	1
NRL	Washington, D. C.	R. E. Seely	1
Facility			
NOTS	China Lake, Calif.	W. J. Werback	1
U. S. GOVERNMENT AGENCIES			
NASA	Greenbelt, Md.	J. C. New	1
		J. Boeckle	1
		A. R. Timmons	1
Library of Congress	Washington, D. C.	Dr. E. Wenk, Presidential Assistant	1
UNIVERSITIES			
Iowa State Univ., Nuclear Eng. Dept.	Ames, Iowa	Dr. G. Murphy	1
Georgia Inst. of Tech., Dept. of Civil Eng	Atlanta, Ga.	Dr. W. M. Sangster	1
Univ. of Missouri, College of Eng.	Columbia, Mo.	Prof. K. H. Evans	1
Catholic Univ., College of Eng.	Washington, D. C.	Dean D. E. Marlowe	1
Notre Dame Univ., College of Eng.	South Bend, Ind.	Dr. J. Hogan	1
CONTRACTORS			
Bendix Missile Systems Div., Dept. 838	400 So. Beiger St. Mishawaka, Ind.	Dr. J. J. Toal	1
McDonnell-Douglas Aircraft Corp.	St. Louis, Mo.	O. McBee	1
Ling-Temco-Vought, Aircraft & Missile Div.	Dallas, Texas	A. Murphy	1
Corning Glass Works	Corning, N. Y.	G. Tatnell	1
		R. Wasson	1

Requests for copies of this report from DoD activities and contractors should be directed to DDC, Cameron Station, Alexandria, Virginia 22314 using DDC Form 1 and, if necessary, DDC Form 55.

*Initial distribution of this document within the Applied Physics Laboratory has been made in accordance with a list on file in the APL Technical Reports Group.

UNCLASSIFIED
Security Classification

DOCUMENT CONTROL DATA - R & D

Security classification of title, body of abstract and indexing annotation must be entered when the overall report is classified)

1 ORIGINATING ACTIVITY (Corporate author) The Johns Hopkins Univ., Applied Physics Lab. 8621 Georgia Ave. Silver Spring, Md. 20910	2a. REPORT SECURITY CLASSIFICATION Unclassified 2b. GROUP N. A.

3 REPORT TITLE

Temperature Functions for Ogival Radome Thermal-Stress Analysis

4 DESCRIPTIVE NOTES (Type of report and inclusive dates)

Technical Memorandum

5 AUTHOR(S) (First name, middle initial, last name)

Manford B. Tate

6 REPORT DATE August 1968	7a. TOTAL NO. OF PAGES 15	7b. NO. OF REFS 7
8a. CONTRACT OR GRANT NO. NOw 62-0604-c b. PROJECT NO c. d.	9a. ORIGINATOR'S REPORT NUMBER(S) TG-1008 9b. OTHER REPORT NO(S) (Any other numbers that may be assigned this report)	

10. DISTRIBUTION STATEMENT

This document has been approved for public release and sale; its distribution is unlimited.

11. SUPPLEMENTARY NOTES	12. SPONSORING MILITARY ACTIVITY NAVORDSYSCOM ORD-03511, Zip 20390

13. ABSTRACT

→ Nine temperature functions are required in finding thermal stresses in the main body of a bicentric-ogive radome, and seven in the nosecap. They are formulated and collected in this report for future use in numerical analysis. Of these nine functions, the following are discussed, exemplified, and evaluated numerically:

(1) Spanwise distribution of temperature along the outer surface of the radome,

(2) Temperature distribution through the thickness of the radome wall,

(3) Zonal distributions of thermal strain,

(4) Thermal normal-stress resultants,

(5) Thermal bending-moment resultants,

DD FORM 1 NOV 65 1473

UNCLASSIFIED
Security Classification

14.

KEY WORDS

Thermal stress analysis
Radome temperature functions
Empirical temperature functions
Numerical temperature functions